Molecular Crystals and Liquid Crystals

ISSN: 1542-1406 (Print) 1563-5287 (Online) Journal homepage: http://www.tandfonline.com/loi/gmcl20

Angular multiplexing of holographic display using tunable multi-stage gratings

Zhonglin Zhang, Chao Ping Chen, Yang Li, Bing Yu, Lei Zhou & Yishi Wu

MOLECULAR CRYSTALS AND LIQUID CRYSTALS
2017, VOL. 657, 102–106
https://doi.org/10.1080/15421406.2017.1403787

Angular multiplexing of holographic display using tunable multi-stage gratings

Zhonglin Zhang, Chao Ping Chen, Yang Li, Bing Yu, Lei Zhou, and Yishi Wu

Smart Display Lab, Department of Electronic Engineering, Shanghai Jiao Tong University, Shanghai, China

ABSTRACT
A holographic display using tunable multi-stage gratings for angular multiplexing is proposed. Using a liquid crystal waveguide and cascaded gratings, it could continuously steer light in a large range and modulate light intensity in every direction, facilitating wide-viewing-angle holographic displays. Furthermore, because of the compact design and micron-level size, it is feasible to integrate this structure into flat-panel display devices and other applications.

KEYWORDS
Angular multiplexing; grating; holographic display; spatial light modulator

1. Introduction

Holographic display is known as a genuine three-dimensional (3D) display in that both the amplitude and phase of light can be reconstructed [1–10]. However, the development of holographic display has been being cursed by several technical obstacles. Among other things, the viewing angle of holographic display is greatly limited by the pixel size of the spatial light modulator (SLM) [11–13]. For example, when the pixel size of SLM is 3.74 μm, the maximum viewing angle for the wavelength of 550 nm is only 8.4°. Hence, in order to widen the viewing angle, a SLM with a sub-wavelength pixel size is favored. But the fabrication of such SLMs requires a highly sophisticated process at a tremendously raised cost.

In this paper, we propose an alternative pixel structure of SLM for holographic display, which is highlighted by a planar waveguide filled with liquid crystal (LC) and multi-stage rectangular gratings. By electrically tuning the refractive index of LC, the direction of the light emerging from the waveguide can be controlled within a broad range. In what follows, its operational principle, simulation results and potential problems are to be elaborated.

2. Operational principle

The proposed pixel structure and its operational principle are depicted in Fig. 1. The multi-stage rectangular gratings are fabricated on the inner surface of the bottom substrate. On the top substrate is coated a common non-patterned electrode. On the bottom substrate is coated patterned multi-stage electrodes. The spacer is responsible for maintaining the cell gap. Between two substrates is sandwiched a layer of nematic LC, whose directors are homogeneously aligned with the grating grooves. The refractive index of gratings should match

CONTACT Chao Ping Chen ccp@sjtu.edu.cn Smart Display Lab, Department of Electronic Engineering, Shanghai Jiao Tong University, Shanghai, China.
Color versions of one or more of the figures in the article can be found online at www.tandfonline.com/gmcl.

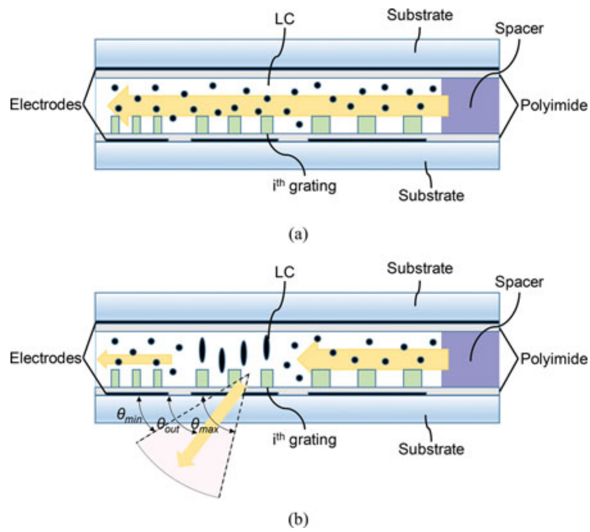

Figure 1. The proposed pixel structure when (a) null voltage is applied, and (b) a voltage is applied to the ith grating.

with the extraordinary refractive index n_e of LC, which is higher than that of the substrate. By doing so, a planar waveguide can be formed for the s-polarized light as the refractive index it encounters within the waveguide is greater than that of the substrate. When a voltage is applied between the common electrode and one of the multiple stage electrodes, say the ith electrode, as shown in Fig. 1(b), LC molecules above the ith electrode will be tilted along the electric filed, giving rise to a mismatch between the refractive indices of LC and grating. As a result, the s-polarized light will be coupled out of the waveguide at an angle θ, which is given by [14]

$$\cos(\theta) = n_{eff} - \lambda/\Lambda_i \tag{1}$$

where n_{eff} is the effective refractive index of LC, λ is the wavelength, and Λ is the period of ith grating. The effective refractive index n_{eff} can be tuned by the applied voltage according to

$$n_{eff}(V) = \sqrt{n_{eff0}^2 - n_e^2 + s \cdot n_g^2 + (1 - s)\, n_i^2(V)} \tag{2}$$

where n_{eff0} is the initial effective refractive index, for which a propagation mode is generated prior to entering the region of the ith grating, s is the ratio of the thickness of the grating to that of the bulk region, n_g is the refractive index of grating, and $n_i(V)$ is refractive index of LC of region of the ith grating. From Eqs. (1) and (2), it can be seen that, for the ith grating, there is an angular range between θ_{min}^i and θ_{max}^i, for which the s-polarized light could be coupled out. In order for the angular ranges of two adjacent gratings to be overlapped, the following condition shall be satisfied

$$\theta_{max}^i \geq \theta_{min}^{i+1} \tag{3}$$

Therefore, through the angular multiplexing of multi-stage gratings, a wide-angle holographic display can be realized. Besides, the light intensity is also tunable using a driving scheme known as pulse width modulation (PWM) [15]. For an accurate PWM, a small cell gap is preferred as the response time of LC is inversely proportional to the cell gap [16].

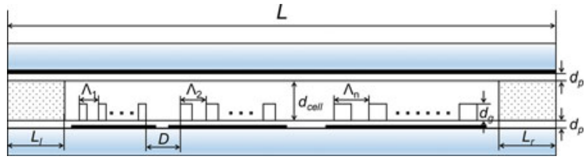

Figure 2. The schematic structure of the simulation model.

3. Results and discussion

Our simulation is implemented with the softwares COMSOL Multiphysics, in which the interface of electromagnetic waves (frequency domain) is employed, and DIMOS.2D. The former, based on the finite element method (FEM) [17], is capable of analyzing the distribution of electric field, out-coupling direction, and intensity of far-field radiation. The latter, also based on FEM, is used to calculate the profiles of electric fields and LC directors. The design wavelength is 488 nm. Figure 2 is a schematic drawing of our simulation model, where rectangular gratings of different periods are created and the light is coupled in from the right side and coupled out by the selected stage grating. Table 1 lists the parameters used for the simulation. The total length of the pixel is 233.9 μm.

Figure 3 shows the directions of out-coupled light with respect to the effective refractive index under different conditions of stage gratings. The solid lines denote the results calculated using Eq. (1), while the circles the results calculated by COMSOL. For a continuous modulation, the maximum out-coupling direction of one stage grating shall overlap with the minimum of out-coulping direction of the next stage grating.

Figure 4 shows the angular-dependent intensity of far-field electric field. Light is radiated in the direction of about 86°. A strict angular selectivity is observed as the beam width of 3 dB is only 0.8°, which is attributed to a relatively small leakage constant [18].

Table 1. Parameters used in the simulation.

Object	Parameter	Symbol	Value
Incident light	Wavelength	λ	488 nm
Substrate	Refractive index	n_s	1.463
LC[a]	Cellgap	d_{cell}	400 nm
	Extraordinary refractive index	n_e	1.775
	Ordinary refractive index	n_o	1.534
	Parallel dielectric constant	$\varepsilon_{//}$	20
	Perpendicular dielectric constant	$\varepsilon_{\perp}$	7
	Splay elastic constant	K_{11}	12.5 pN
	Twist elastic constant	K_{22}	7.3 pN
	Bend elastic constant	K_{33}	17.9 pN
Polyimide	Thickness	d_p	80 nm
	Refractive index	n_p	1.59
Grating	Thickness	d_g	100 nm
	Period of the 1st stage	Λ_1	318.6 nm
	Period of the 2nd stage	Λ_2	331.2 nm
	Period of the 3rd stage	Λ_3	343.7 nm
	Period of the 4th stage	Λ_4	358.2 nm
	Period of the 5th stage	Λ_5	374.9 nm
	Period of the 6th stage	Λ_6	392.6 nm
	Spacing between two gratings	D	2 μm
	Number of gratings for each stage	N	100
Dimension	Total length	L	233.9 μm
	Length of right end	L_r	5 μm
	Length of left end	L_l	5 μm

[a]Parameters of E7 are adopted.

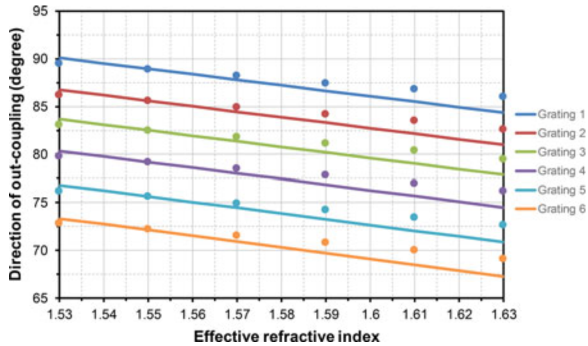

Figure 3. Direction of out-coupled light with respect to the effective refractive index under different conditions of stage gratings.

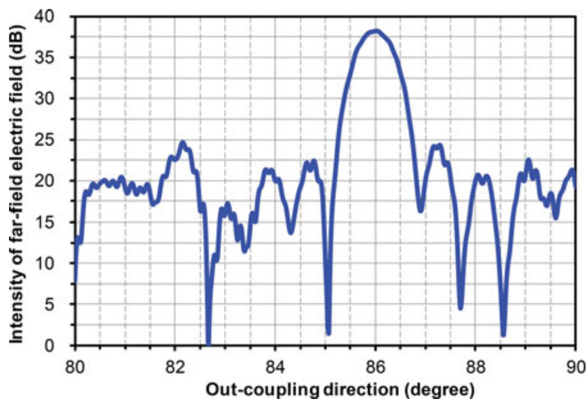

Figure 4. The dependence of intensity of far-field electric field on the out-coupling direction.

Figure 5 plots the dependency of diffraction efficiency (DE)—defined as the ratio of the power of out-coupled light to that of incident light—on the effective refractive index n_{eff} of LC. It can be noticed that DE drops when n_{eff} increases, which is the result of the reduced refractive index modulation between LC and the grating. Assuming that the minimum acceptable DE is 10%, the maximum n_{eff} shall be 1.63. Hence, the effective refractive index of LC is tunable between 1.53—i.e. LC's ordinary refractive index—and 1.63. When n_{eff} varies from 1.53 to 1.63, θ will accordingly change from 69.0° to 89.5°, forming a 20.5° viewing cone. If the light could be emitted from the opposite direction as well, the entire viewing cone will be doubled to 41°.

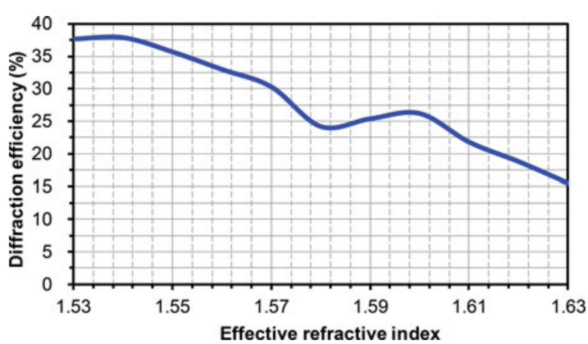

Figure 5. Diffraction efficiency as a function of the effective refractive index of the LC layer.

4. Conclusions

A pixel structure of SLM for holographic display, which is highlighted by a planar waveguide filled with LC and multi-stage rectangular gratings, is proposed. By electrically tuning the refractive index of LC, the direction of the light emerging from the waveguide can be controlled within a wide angular range of 20.5°. If the light could be emitted from both right and left sides, the entire viewing cone will be doubled to 41°.

Funding

This work is supported by Ministry of Science and Technology of the People's Republic of China (2013CB328804, 2015AA017001), Shanghai Jiao Tong University (AF0300204, WF101103001/085), and Shanghai Rockers Inc. (15H100000157).

References

[1] Tay, S., Blanche, P.-A., Voorakaranam, R., Tunc, A. V., Lin, W., Rokutanda, S., Gu, T., Flores, D., Wang, P., Li, G., St. Hilaire, P., Thomas, J., Norwood, R. A., Yamamoto, M., & Peyghambarian, N. (2008). *Nature*, *451*(7179), 694–698.
[2] Yaras, F., Kang, H., & Onural, L. (2010). *J. Disp. Technol.*, *6*(10), 443–454.
[3] Toal, V. (2011). *Introduction to Holography*, CRC Press: Boca Raton, FL.
[4] Smalley, D. E., Smithwick, Q. Y. J., Bove Jr., V. M., Barabas, J., & Jolly, S. (2013). *Nature*, *498*(7454), 313–317.
[5] Xiong, Y., He, Z., Chen, C. P., Li, X., Li, A., Ye, Z., Lu, J., He, G., & Su, Y. (2013). *Opt. Commun.*, *296*, 41–46.
[6] Li, X., Chen, C. P., Gao, H., He, Z., Xiong, Y., Li, H., Hu, W., Ye, Z., He, G., Lu, J., & Su, Y. (2014). *J. Disp. Technol.*, *10*(6), 438–443.
[7] Li, X., Chen, C. P., Li, Y., Jiang, X., Li, H., Hu, W., He, G., Lu, J., & Su, Y. (2014). *Chin. Opt. Lett.*, *12*(6), 060003.
[8] Chen, C. P., Su, Y., & Jhun, C. G. (2014). *J. Opt. Photonics*, *1*, 1–8.
[9] Hu, W., Chen, C. P., Li, Y., He, Z., Li, X., Zhou, P., Lu, J., & Su, Y. (2015). *Opt. Express*, *23*(4), 4726–4735.
[10] Li, X., Chen, C. P., Li, Y., Zhou, P., Jiang, X., Rong, N., Liu, S., He, G., Lu, J., & Su, Y. (2016). *J. Disp. Technol.*, *12*(4), 362–367.
[11] Stanley, M., Smith, M. A. G., Smith, A. P., Watson, P. J., Coomber, S. D., Cameron, C. D., Slinger, C. W., & Wood, A. D. (2004). *Proc. of SPIE*, *5249*, 297–308.
[12] Buckley, E., Cable, A., Lawrence, N., & Wilkinson, T. (2006). *Appl. Opt.*, *45*(28), 7334–7341.
[13] Hahn, J., Kim, H., Lim, Y., Park, G., & Lee, B. (2008). *Opt. Express*, *16*(16), 12372–12386.
[14] Schwering, F. K., & Peng, S.-T. (1983). *IEEE Trans. Microw. Theory Tech. MTT*, *31*(2), 199–209.
[15] Cristaldi, D. J. R., Pennisi, S., & Pulvirenti, F. (2009). *Liquid Crystal Display Drivers: Techniques and Circuits*, Springer.
[16] Wu, S.-T., & Yang, D.-K. (2001). *Reflective Liquid Crystal Displays*, Wiley: Chichester, UK.
[17] Pepper, D. W., & Heinrich, J. C. (2017). *The Finite Element Method: Basic Concepts and Applications with MATLAB, MAPLE, and COMSOL*, 3rd Edition, CRC Press: Boca Raton, FL.
[18] Song, Q., Campione, S., Boyraz, O., & Capolino, F. (2011). *Opt. Express*, *19*(9), 8735–8749.